Int. J. Multiphase Flow Vol. 16, No. 2, pp. 187–200, 1990
Printed in Great Britain. All rights reserved

0301-9322/90 $3.00 + 0.00
Copyright © 1990 Pergamon Press/Elsevier

WAKE SOLIDS HOLDUP CHARACTERISTICS BEHIND A SINGLE BUBBLE IN A THREE-DIMENSIONAL LIQUID–SOLID FLUIDIZED BED

B. E. KREISCHER, H. MORITOMI and L.-S. FAN†
Department of Chemical Engineering, The Ohio State University, Columbus, OH 43210, U.S.A.

(*Received* 11 *April* 1989; *in revised form* 25 *September* 1989)

Abstract—A light transmittance technique using a dual optical fiber probe was used to measure the local solids holdup in a three-dimensional gas–liquid–solid fluidized bed. The bubble can be clearly identified in the same signal, thus permitting the simultaneous determination of the local solids holdup profile in the wake of a single bubble and the rise velocity and chord length of the bubble. The solid holdup behavior was studied in the wake of single bubbles rising in a liquid–solid fluidized bed for different liquid velocities, particle sizes and bubble sizes. Over the range investigated in this study, the wake solids holdup was found to decrease with decreasing mean solids holdup in the bed, to depend only slightly on bubble Reynolds number and to decrease with increasing particle size.

Key Words: bubble wake, solids holdup, three-phase fluidization, single bubble, optical fiber probe, gas–liquid–solid systems, fluidized bed

INTRODUCTION

Gas–liquid–solid fluidization offers many advantages for application to a variety of industrial reactions (Fan 1989). Applications may range from fermentation and wastewater technology to the hydrotreating of petroleum residue. These widely different applications involve significantly different bubble behavior and, consequently, different mass and heat transfer behavior. The understanding of bubble and bubble wake characteristics in three-dimensional beds is essential to a fundamental understanding of the bed hydrodynamics.

Bubble sizes are measured typically by either photographic or probe techniques. Probe techniques are particularly suitable for three-dimensional beds. Optical fiber techniques for measuring bubble properties in three-phase fluidized beds have been developed that detect either reflected (e.g. Abauf *et al.* 1978; Ishida & Tanaka 1982; de Lasa *et al.* 1984; Hu *et al.* 1986; Kitano & Fan 1988) or transmitted light (Kitano & Fan 1988). The light transmittance method developed by Kitano & Fan (1988) can detect the local solids holdup behavior in a two-dimensional gas–liquid–solid fluidized bed.

Most published research on bed hydrodynamics deals with the measurement and prediction of the individual phase volume fractions at various flow conditions (e.g. Bhatia & Epstein 1974; Dhanuka & Stepanek 1978; Michelsen & Ostergaard 1970; Bhaga & Weber 1972). Several models for predicting the volume fractions have been presented in which the bubble wake has been recognized as a primary factor (Darton & Harrison 1975; Bhatia & Epstein 1974; El-Temtamy & Epstein 1978; Jean & Fan 1987). In these models, a gas–liquid–solid fluidized bed is considered to consist of a bubble (gas) phase, a wake phase and a particulate (liquid–solid fluidized) phase; in addition, the wake phase is assumed to travel with the bubble at the bubble rise velocity. However, the wake phase has been considered to be both solids-free or solids-containing.

In the generalized form of the wake model, the wake-to-bubble volume ratio, K, and the ratio of the solids holdup in the wake phase to that in the particulate phase, X, express the wake properties. As described by Kitano & Fan (1988), these parameters have been evaluated empirically, but indirectly, or through theoretical developments based upon physical insight

†To whom all correspondence should be addressed.

(Hetzler & Williams 1969; Henriksen & Ostergaard 1974; El-Temtamy & Epstein 1978). El-Temtamy & Epstein (1978) proposed the equation

$$X = 1 - 0.877\frac{U_t}{U_b} \qquad [1]$$

as a correlation for X in terms of bubble and particle properties. In [1], U_t and U_b are the particle terminal velocity and relative bubble rise velocity, respectively. Systematic direct measurements of wake size and wake solids concentrations are limited and a fundamental understanding of the two parameters is lacking.

Investigations of the wake phase from a fundamental viewpoint have been reported recently. Tsuchiya & Fan (1988) investigated the wake structure of a single gas bubble in a liquid–solid fluidized bed through visualization; they identified a primary wake region based on the fluid mechanical structure of the wake. Kitano & Fan (1988) examined the wake structure in terms of both bubble wake size and average solids holdup behavior using a combination of optical fiber probe and visual techniques. In both studies, a two-dimensional bed was used to facilitate visualization. Based on direct measurement, Kitano & Fan (1988) reported the solids holdup in an "effective" wake region to be a constant around 0.42 regardless of bubble size, particle size, particle properties and liquid velocity. The effective wake region considered by Kitano & Fan (1988), in essence, corresponds to the confined turbulent wake region (Fan 1989) which is smaller than the primary wake region defined by Tsuchiya & Fan (1988). In addition, Kitano & Fan (1988) found the wake size to be almost independent of bubble Reynolds number (Re_b) between 4000 and 10,000 with the average wake-to-bubble volume ratio being about 2.8: in this case Re_b is defined as $\rho_L U_b D_e/\mu_L$, where ρ_L is the liquid density, D_e is the sphere-equivalent bubble diameter and μ_L is the liquid viscosity. Miyahara *et al.* (1988) studied the wake size and vortex shedding behavior in a three-dimensional bed with low solids concentrations; they found an average value of the wake-to-bubble volume ratio of 2.5 over a wide range of Re_b.

This study complements previous studies of the wake behavior by investigating the local solids holdup behavior behind a single bubble rising in a three-dimensional liquid–solid fluidized bed. An optical fiber probe technique is used to measure both the local solids holdup and bubble characteristics in a three-dimensional bed. Examination of the local solids holdup profile leads to the direct evaluation of X.

EXPERIMENTAL

The basic experiment in this study was to inject a single gas bubble into a liquid–solid fluidized bed. The system used, which is described in detail in Miyahara *et al.* (1988), was a 102 mm i.d. acrylic column 1.6 m high with a perforated plate liquid distributor. Individual nitrogen bubbles were injected into beds of glass beads fluidized by water at a given liquid velocity. The volume of glass beads used was varied to maintain a constant bed height and the bubble size was controlled by adjusting the injection pressure (P_i) and the electrical pulse width sent to a solenoid valve. Glass beads 163, 326, 460 and 760 μm dia were used extensively in this study. Table 1 lists the density (ρ_p) and terminal velocity (U_t) for each particle size. The liquid velocity was varied to provide mean solids holdups in the liquid–solid fluidized bed ($\bar{\epsilon}_s$) between 0.06 and 0.51.

Two important experimental techniques were used in this study. (1) A video system recorded observations of bubbles emerging from the bed surface. From these observations, a bubble size could be calculated based on the projected area of the rising bubble. (2) The second light transmittance method of Kitano & Fan (1988) was adapted into an intrusive light transmittance

Table 1. Particle properties pertinent to the study

Particles	ρ_p (kg/m^3)	U_t (m/s)	n[a]
163 μm glass	2.52×10^3	1.7×10^{-2}	4.05
326 μm glass	2.52×10^3	4.4×10^{-2}	3.46
460 μm glass	2.50×10^3	6.8×10^{-2}	3.21
760 μm glass	2.50×10^3	1.18×10^{-1}	2.93

[a]Richardson–Zaki index (Richardson & Zaki 1954).

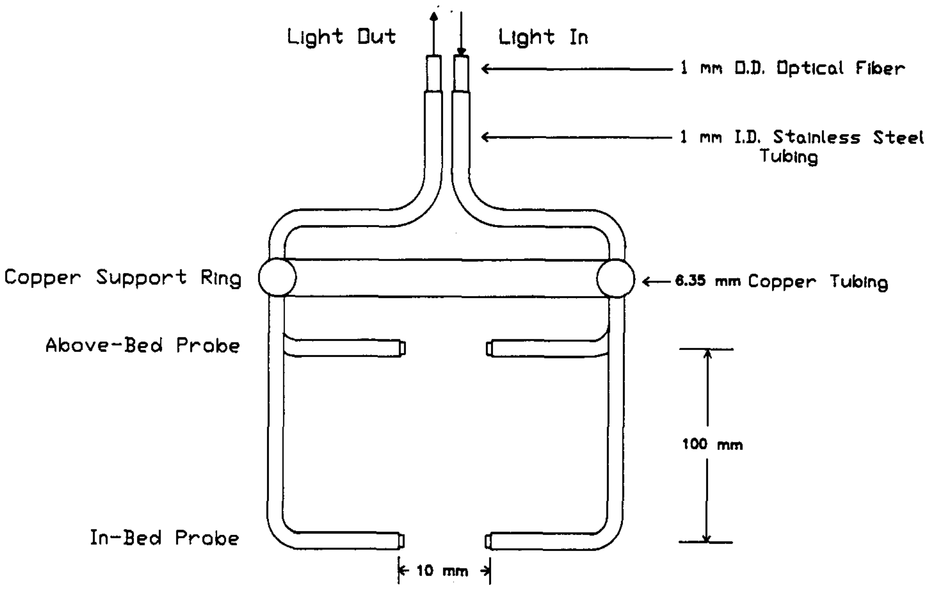

Figure 1. Drawing of the dual optical fiber probe and the copper tubing support ring assembly. The measurement zone for each probe is 10 mm.

probe assembly to measure the bubble size, bubble rise velocity and the local solids holdup within the bubble wake.

The light transmittance probe assembly contained two individual probes separated by a fixed vertical distance. The probe assembly was positioned so that the upper probe was located 10 mm above the bed surface (0.8 m above the distributor plate). The individual probes consisted of two optical fibers supported by stainless steel tubing: one fiber transmits light from a light source to the measurement zone, while the other receives light from the measurement zone and sends it to a photomultiplier tube. Figure 1 gives a schematic diagram of the actual probe. The optical fibers in each probe were 1.0 mm dia and separated by a 10 mm measurement zone. A distance of 0.10 m separated the individual probes. The stainless steel support tubes had 1.0 mm i.d. and the copper mounting ring was made from 6.35 mm pipe.

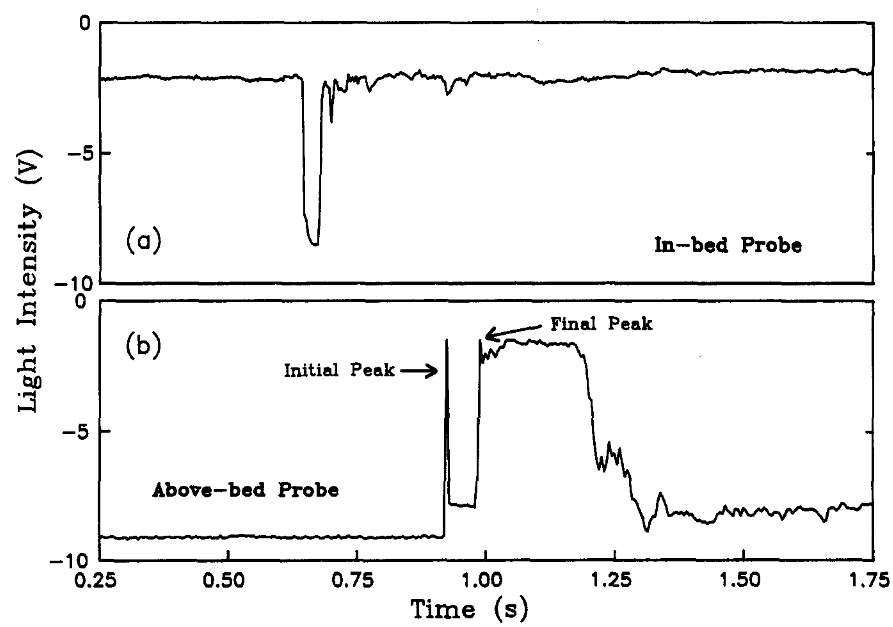

Figure 2. Typical voltage output signals from the photomultiplier tube for both the in-bed and above-bed probes.

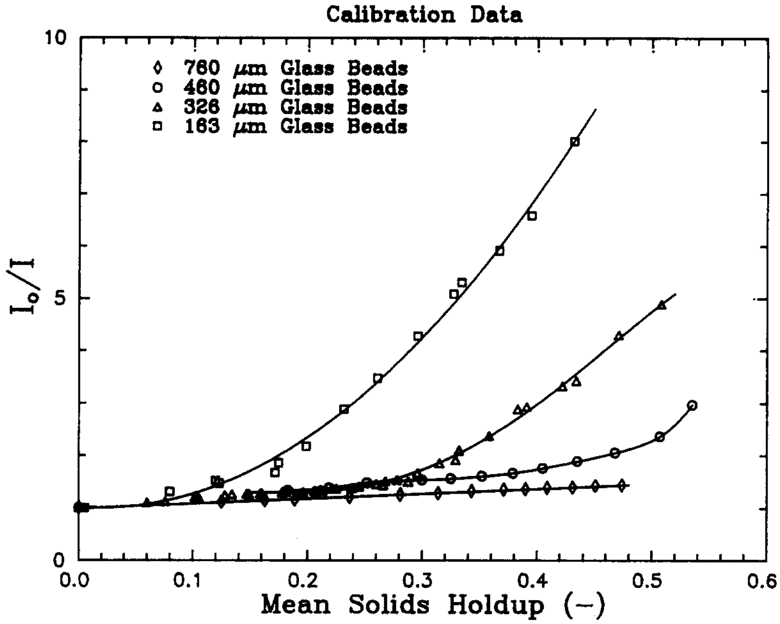

Figure 3. System opacity as a function of the mean solids holdup and particle size. Note the decrease in probe sensitivity with increasing particle size.

The photomultiplier, which was connected to a voltage divider circuit driven by a variable high voltage (d.c.) source, converted the intensity of the light obtained from the probe into a voltage between + 10 and − 10 V. The analog voltage signal was then digitized by a Micro-Byte Dash-16 A/D converter at a fixed sampling rate and stored in an IBM PC-XT.

For a single large bubble, typical output signals from the photomultiplier are given in figures 2(a, b). Figure 2(a) is from the in-bed probe, while figure 2(b) is from the above-bed probe. The characteristic signal for the bubble can be identified in each signal. The bubble rise velocity can be calculated by dividing the 0.10 m distance separating the two probes by the time elapsed between when the bubble first passes the in-bed probe and when it first passes the above-bed probe. These signals represent the raw data for the experiments. The raw data must be converted to solids holdup.

The basis for the local solids measurements is that the intensity of light absorbed in passing through a measurement zone will depend on the solids holdup in that zone. The Lambert–Beer law, slightly rearranged, expresses the solution opacity (O_p) in terms of the solute concentration:

$$O_p = \frac{I_0}{I} = \exp(\alpha C x), \qquad [2]$$

where I is the measured transmitted light intensity, I_0 is the light intensity transmitted through the solvent alone, α is the absorption coefficient, C is the solute concentration and x is the thickness of the absorption cell. As an approximation, [2] can be extended to a liquid–solid medium by replacing the solute concentration with the solids holdup (ϵ_s). This approach was valid at low solids holdups, but, as indicated by Kitano & Fan (1988), does not extend well to the full range of solids concentrations.

Since the Lambert–Beer law failed to adequately describe the opacity behavior over the entire solids holdup range, a simple calibration was used. The procedure involved two main steps: first, the intensity of light passing through a liquid medium (I_0) was measured; and second, for a given mean solids holdup, the light intensity was measured as a function of time and then averaged. The second step in the procedure was conducted for various mean solids holdups.

Figure 3 shows the average opacity vs mean solids holdup for liquid–solid fluidized beds of 163, 326, 460 and 760 μm dia glass beads. As illustrated, the 163 μm glass beads show the greatest increase in opacity with increasing solids holdup; the 326 μm glass beads show a lesser increase, as do the 460 and 760 μm glass beads. Each particle size shows similar opacity behavior: at low

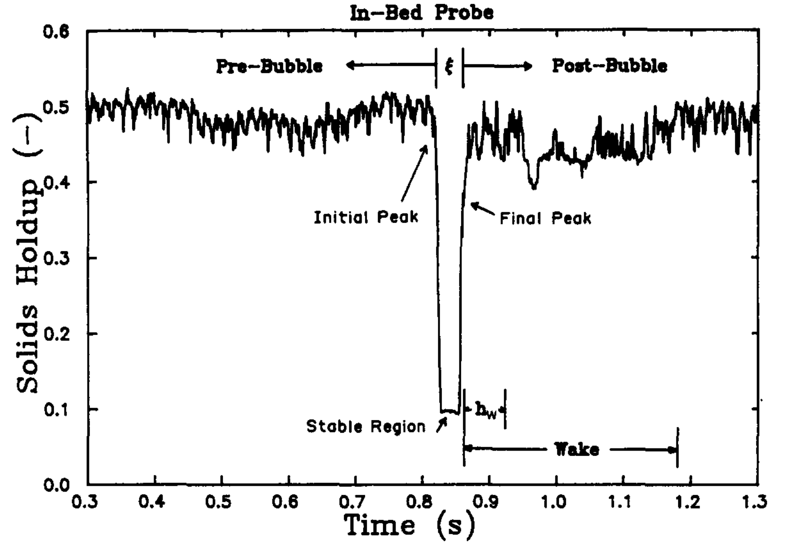

Figure 4. Typical local solids concentration signal subdivided into the pre-bubble, the bubble and the post-bubble regions.

solids holdup the opacity increases almost linearly with means solids holdup while at large solids holdup the slope becomes much greater. The probe sensitivity towards the solids holdup can be quantified for each particle size through the change in opacity with mean solids holdup.

RESULTS AND DISCUSSION

The technique for measuring the local solids holdup provides local solids holdup data prior to, during and after the passing of the bubble. Figure 4 presents a representative local solids holdup profile and identifies the regions and parameters important to the analysis of the data. The signal is subdivided into the pre-bubble (prior to passing), the bubble and the post-bubble (after passing) regions.

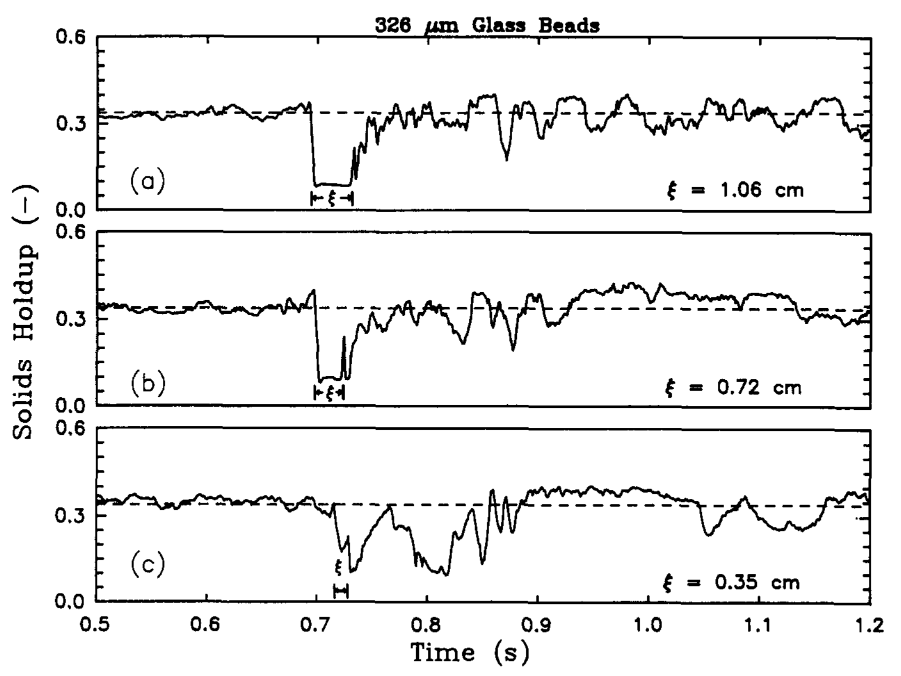

Figure 5. Solids holdup measurements behind single bubbles created under identical conditions (note the sampling rate for these data is 100/s).

The pre-bubble region, typically, shows high frequency fluctuations or noise characteristics of both the probe and particle size dimensions. In addition, depending on the flow conditions, global variations can be identified which depend on the hydrodynamic conditions within the bed: these global variations should depend on particle size and reflect the bed hydrodynamics.

In the bubble region, the value of the solids holdup is meaningless. Ideally, the bubble can be identified as two characteristic peaks separated by a stable region of high intensity [e.g. see figure 2(a)]. This stable region corresponds to the transmission of light through nitrogen. The peaks represent a sharp decrease in light transmission followed immediately by a sharp increase: the decrease in transmission in the initial peak or the increase in the final peak may be masked if the mean solids holdup is high (e.g. see figure 4). The bubble chord length (ξ) was defined as the time difference between when the apex of the initial peak and the apex of the final peak occur multiplied by the bubble rise velocity. At high mean solids holdups, the chord length is based on the initial point of sharp increase and the final point of sharp decrease in intensity coming after the stable high transmittance region.

The post-bubble region starts after the bubble base peak and continues to the end of the signal. This region consists of the wake (both primary and secondary), and, in some cases, a zone of stable liquid–solid fluidization. Generally, the wake has solids holdup variations larger than those found in the pre-bubble region.

The local solids holdup variations in the wake can be analyzed both qualitatively and quantitatively to provide insight into the wake structure. Quantitative analysis of the average wake solids holdup based on these signals requires determination of the boundary between the primary and secondary wake, since the boundary cannot be distinguished based on the local solids holdup signal by itself.

Three data sets, each corresponding to a single bubble injected under identical conditions, are presented in figures 5(a–c): in this case, $Re_b = 7200$ ($P_i = 30$ psig) and the mean solids holdup was 0.34. As shown, the chord length observed is not the same for each repetition: the signal in figure 5(a) has the largest measured chord length, figure 5(c) the smallest and figure 5(b) falls in between. The differences result because the bubbles do not necessarily strike the probe at the same lateral location for each repetition; consequently, the probe measurements can be used to infer insight into the local solids holdup at different lateral locations within the wake. For bubbles of a given volume, a larger observed chord length suggests the probe passed through the bubble closer to the central axis. The similarity between the wake solids concentration profiles in figures 5(a, b) suggest a near uniform solids concentration region near the central axis. However, in figure 5(c), the signal with the smallest measured chord length, which represents a profile closest to the bubble edge, the concentration varies significantly over a short distance through the wake and from that found in figures 5(a, b).

The behavior pictured in figures 5(a–c) agrees with that found by Kitano & Fan (1988) in two-dimensional beds in that: (i) a stable solids region exists in the wake near the bubble central axis; (ii) close to the bubble edge a vortex sheet region exists: in the stable solids region the solids concentration variations are relatively small, while in the vortex sheet region the solids concentration variations could be relatively large. Also evident in figures 5(a–c), is that solids holdup variations prior to the passing of the bubble are small compared to those found after, the disturbance caused by the passing bubble continues for a significant time and the local solids holdup in the wake can exceed the mean solids holdup. Large-scale solids concentration disturbances like that shown in figure 5(c) may indicate the presence of coherent vortical structure. The location of these disturbances can vary from signal to signal due to the unsteady nature of the vortex shedding process and differences in probe location relative to the bubble central axis.

The experiments in this study were designed to investigate three important properties of a gas–liquid–solid fluidized bed: the mean solids holdup in the bed; the bubble size; and the particle size. The experimental system, however, had limitations on both the bubble and particle sizes which will be indicated by the results.

Figures 6(a–c) show signals for a fluidized bed of 163 μm glass beads typically found over a range of mean solids holdups. At a high holdup ($\bar{\epsilon}_s = 0.50$), measurement of the local solids holdup indicates only a very small change between the data found prior to the passing of the bubble and that following. The sole effect seems to be a very slight decrease in solids holdup [see figure 6(a)].

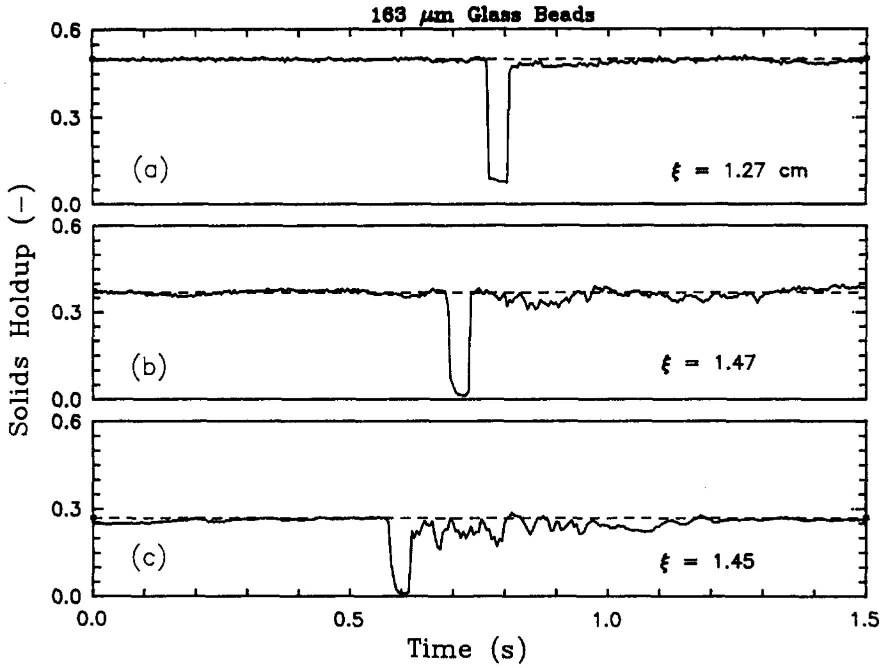

Figure 6. The effect of bed porosity on the local solids holdup in the wake of a single bubble rising in a liquid–solid fluidized bed: (a) 163 μm particles, $\bar{\varepsilon}_s = 0.50$; (b) 163 μm particles, $\bar{\varepsilon}_s = 0.37$; (c) 163 μm particles, $\bar{\varepsilon}_s = 0.27$.

At a lower solids holdup ($\bar{\varepsilon}_s = 0.37$), wake effects begin to become evident: as shown in figure 6(b), in the post-bubble region, the local solids holdup variations begin to increase; the overall pattern seems to be sinusoidal with a long wavelength. At a still lower solids holdup ($\bar{\varepsilon} = 0.27$), the local variations become more intense; as shown in figure 6(c), the wake itself is evident, but a demarcation between the primary and secondary wake is not. Note that at times sufficiently long after the passing of the bubble the solids holdup behavior returns to that found prior to its passing.

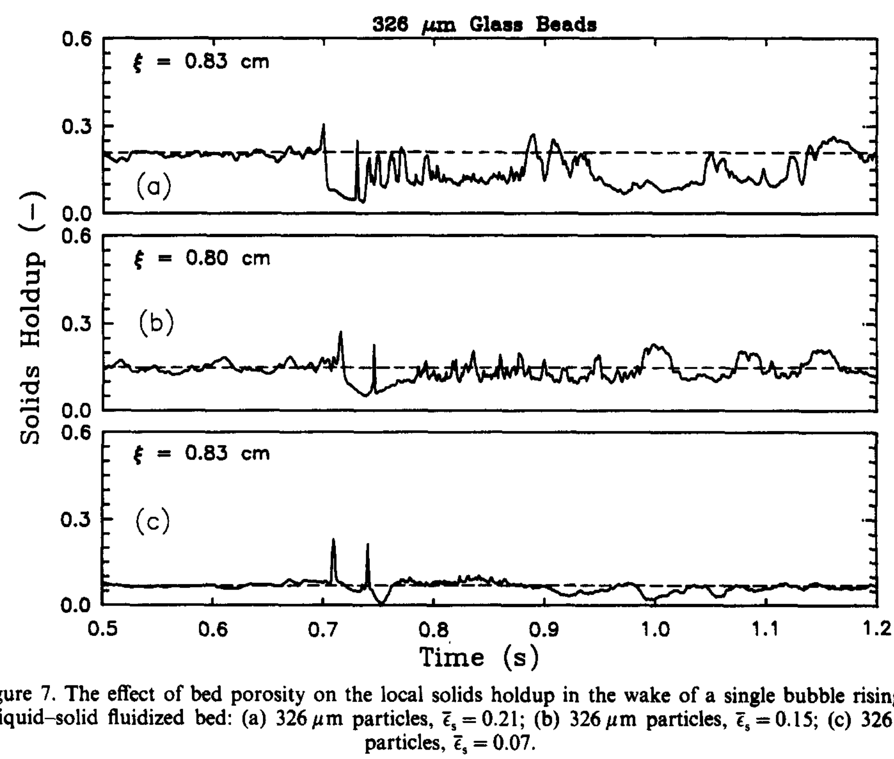

Figure 7. The effect of bed porosity on the local solids holdup in the wake of a single bubble rising in a liquid–solid fluidized bed: (a) 326 μm particles, $\bar{\varepsilon}_s = 0.21$; (b) 326 μm particles, $\bar{\varepsilon}_s = 0.15$; (c) 326 μm particles, $\bar{\varepsilon}_s = 0.07$.

Figures 7(a–c) show typical signals for a fluidized bed of 326 μm glass beads at relatively low solids holdup. In these signals, a low solids concentration region, or liquid wake, exists. In figures 7(a–c) particularly, the spike identifying the bubble base is followed immediately by a low concentration region. Note, however, the low concentration region was not found in all signals for a given set of conditions. Such behavior is in agreement with the observations of Kitano & Fan (1988). The tendency for liquid wakes to exist increased with an increase in particle size and a decrease in mean solids holdup. Also evident in figures 7(a–c) is that at low mean solids holdups the intensity of the solids concentration variations in the wake begins to decrease with decreasing mean solids holdup.

Figures 8(a–d) and 9(a–d) show examples of signals for 163, 326, 460 and 760 μm particles from the in-bed and above-bed probes, respectively. Inside the fluidized bed, the variations in local solids concentration, both in the pre- and post-bubble regions, become larger with increasing particle size. In addition, the intensity of the variations in the wake region increases with increasing particle size. The increase in intensity of the variations stems from both a decrease in probe sensitivity and changes in the hydrodynamic behavior within the bed itself. At higher liquid velocities in the 460 and 760 μm glass bead cases, the large-scale variations can actually mask the passing of the bubble. However, the solids holdup profiles obtained from the above-bed probe show clearly when bubbles pass the probe and thus, these signals remain useful, but are still subject to the decrease in probe sensitivity. The observed solids holdup profile at the above-bed probe contains two important phenomena: at very short times after the passing of the bubble the data should represent the solids carried up from the bed in the wake, while at later times the effect of particle drift from the bed surface becomes important. Note that lower solids concentration regions can also be observed in the above-bed probe signals [see figure 9(d)].

In the determination of the wake boundary, it is desirable to consider that of the primary wake, defined based on the flow pattern in the wake by Tsuchiya & Fan (1988). As noted earlier, Miyahara *et al.* (1988) reported an average value of the ratio of the primary wake volume to the bubble volume of 2.5. For a spherical-cap bubble, this volume ratio yields a value for the relative wake depth (h_w/ξ, where h_w is the wake depth and ξ is the corresponding chord depth) of 2.5. An extensive analysis of the data has revealed that the variation of the average wake solids holdup

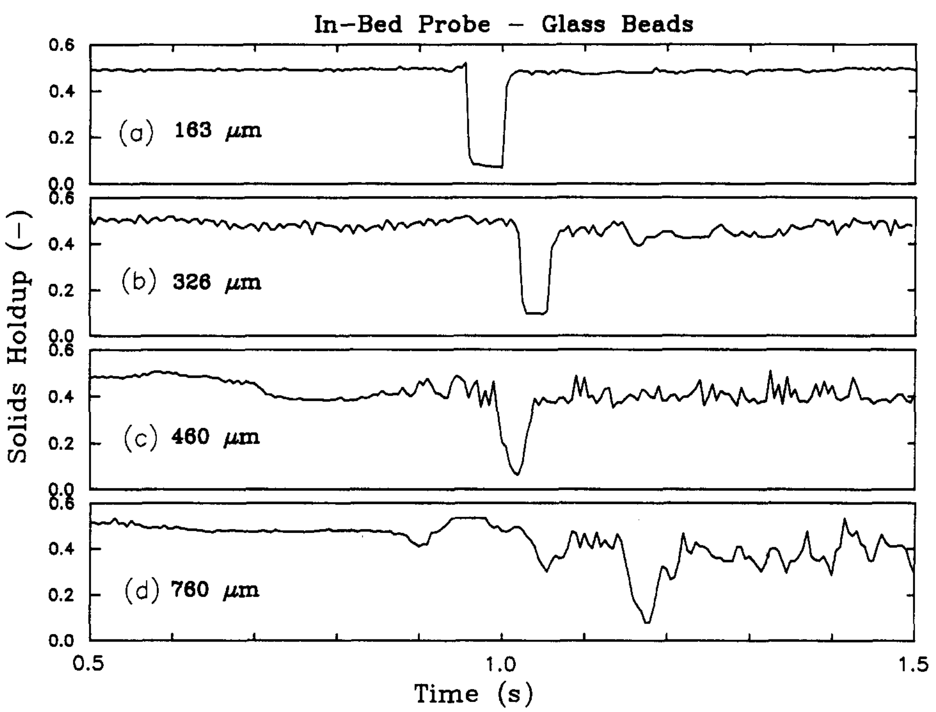

Figure 8. Typical signals from the in-bed probe for 163, 326, 460 and 760 μm glass bead systems (note the sampling rate for these data is 200/s).

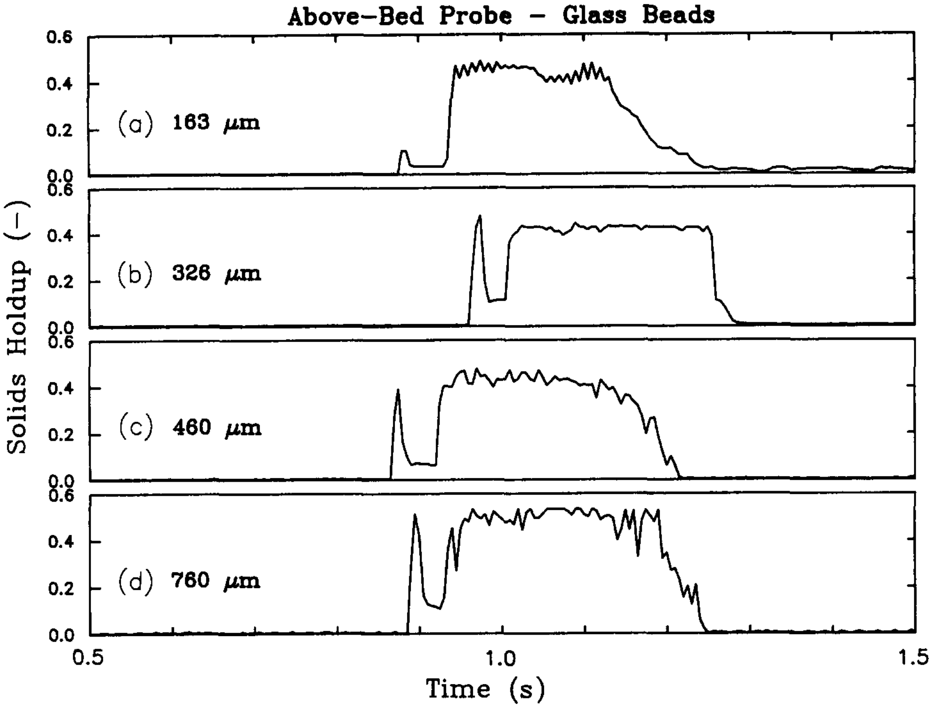

Figure 9. Typical signals from the above-bed for 163, 326, 460 and 760 μm glass bead systems (note the sampling rate for these data is 200/s).

with h_w/ξ in the parametric range of this study is fairly insensitive when h_w/ξ is between 1.5 and 3. The results of the analysis are exemplified in figures 10(a, b) which show the solids concentration in the wake averaged over various prescribed wake sizes, expressed in terms of the relative wake depth, for many single bubbles injected under the same conditions. As shown in figure 10(a), the scatter in the average wake solids holdup, indicated by the error bars, is largest at small wake sizes, but stabilizes at large wake sizes. The scatter is a composite of differences due to variations in location within the wake and also the unsteady state of the wake itself. The mean of the data, as

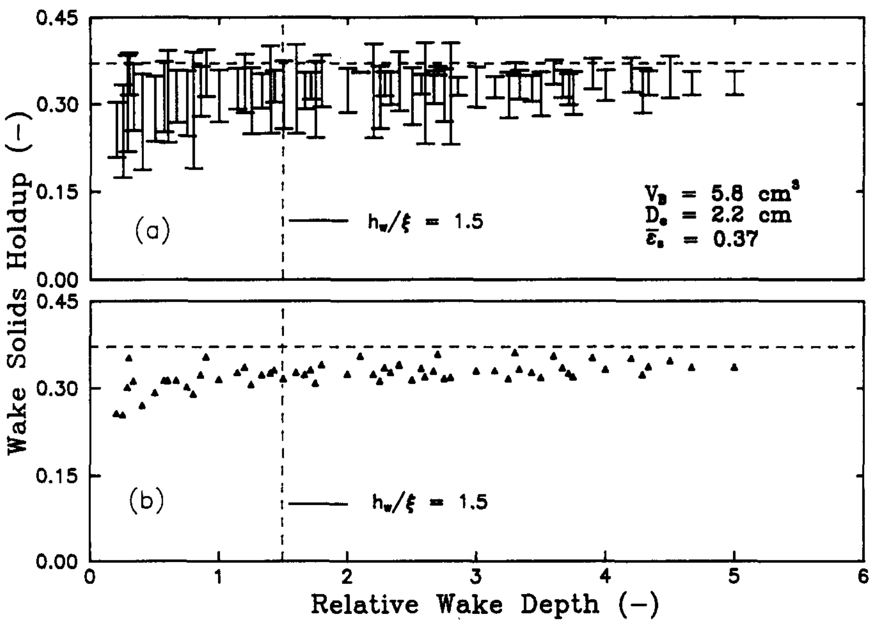

Figure 10. Average wake solids holdup as a function of the relative wake depth: for this study, an h_w/ξ of about 1.5 was used. V_B in (a) is the bubble volume.

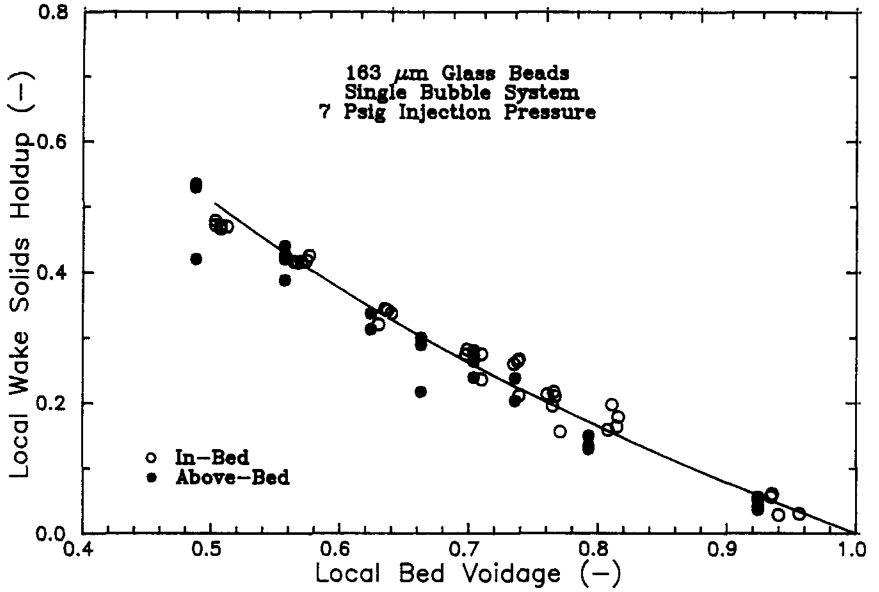

Figure 11. The agreement between wake solids holdup measured in-bed with that measured above-bed as a function of the mean bed voidage in a bed of 163 μm glass beads.

shown in figure 10(b), shows approximately a steady value of 0.33 for h_w/ξ between 1.5 and 3 and progressively approaches the mean solids holdup in the bed, i.e. 0.37, as the wake depth increases. Thus, for practical purposes, a choice of h_w/ξ of 1.5 was used for all conditions in the present calculation.

Since the in-bed signals for the 460 and 760 μm particles showed such a high degree of fluctuations within the bed, while the above-bed signals provide a clear signal, the consistency between the data from these two probes was checked for the smaller size particles to allow the use of the above-bed signals to obtain data for the large particle systems. Average local solids holdup data for individual bubbles taken both by the in-bed and above-bed probes for a bed of 163 μm glass beads are shown in figure 11. Good agreement exists between the data obtained at the different locations not only for the 163 μm glass beads, as shown, but for the 326 μm glass beads as well; since good agreement exists, wake solids holdup data for 460 and 760 μm particles were obtained from the above-bed probe. Due to the inherent unsteady nature of the vortex formation and shedding process, significant scatter exists in the data; therefore, averaging a group of data obtained

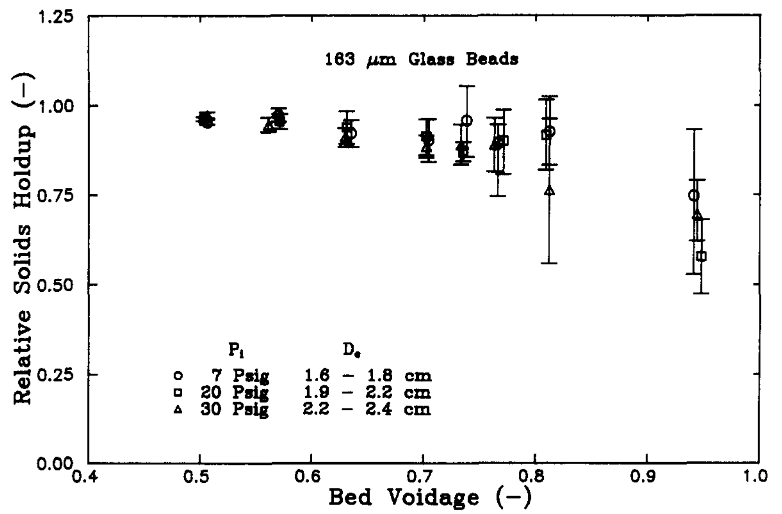

Figure 12. The relative solids holdup vs the mean bed voidage as a function of bubble size in a bed of 163 μm glass beads.

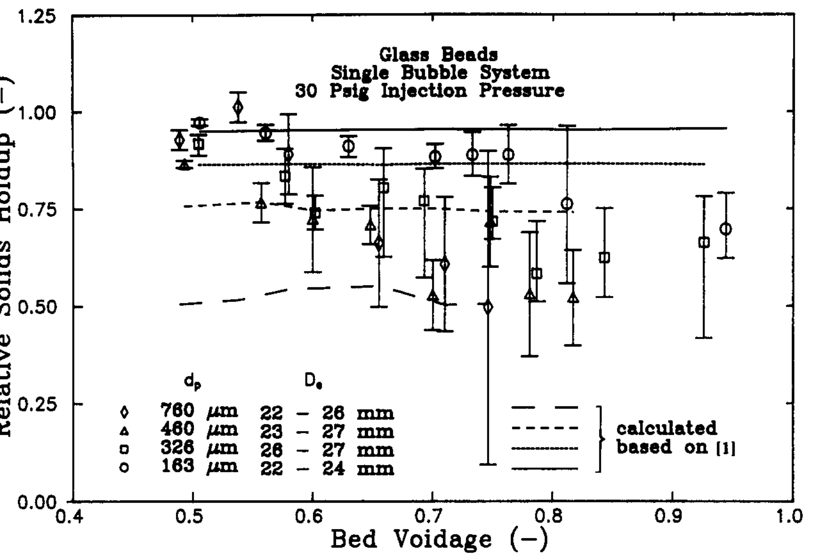

Figure 13. The relative solids holdup vs the mean bed voidage as a function of particle size for a bubble injection pressure of 30 psig.

under identical conditions provides a better estimate of the average solids concentration in the wake region.

The ratio of the solids holdup in the wake to the mean solids holdup, or the relative solids holdup (X), found for 163 μm glass beads for three different bubble sizes is shown in figure 12: the error bars indicate the standard deviation of the data. At a low bed voidage, X is near 1 and the data shows little scatter. For increasing bed voidages, X decreases and the variation in the data increases. As can be seen in the figure, bubble size (bubble injection pressure) only slightly affects the wake solids holdup. Re_b values range from 4200 to 5000 for a 7 psig injection pressure, from 5900 to 7200 for a 20 psig injection pressure and from 7200 to 8200 for a 30 psig injection pressure: note that the variation in Re_b is not directly related to the variation in bed voidage and Re_b has a minor effect on X.

Particle size has a much greater impact on X than the bubble size over the conditions studied. In figure 13, X is shown to decrease as the particle size increases from 163 to 460 μm. Re_b values range from 7200 to 8200 for 163 μm particles, from 7400 to 7800 for 326 μm particles, from 5400 to 6600 for 460 μm particles and from 5200 to 5400 for 760 μm particles, and, once again, no significant direct relationship between the Re_b and X is evident: also, note that the larger fluctuations in solids holdup behavior found in large particle systems are indicated through the size of the error bars. Also shown in figure 13 is the corresponding prediction of El-Temtamy & Epstein's correlation [1] for these data. In the prediction, the experimental values of U_b are used. Clearly, the correlation provides a reasonable prediction of the magnitude of the wake solids holdup, yet does not sufficiently reflect the effect of changing bed voidage.

The measurements and results of this study pertain to spherical-cap bubbles with a volume-equivalent diameter between 1.5 and 3.0 cm and with Re_b in the range 4000–8000. In this range, the wake size as reported in the literature is a relatively weak function of the Re_b (e.g. Tsuchiya & Fan 1988) and the rising motion of the bubble is rectilinear. The rectilinear motion of the rising bubble increases the probability that the bubble will strike the light intensity probe. Particle size and mean solids holdup in the bed affect the bubble motion and hence, should affect the wake solids holdup behavior. The relative motion between both the bubble and the liquid and the bubble and the particles play important roles in the wake behavior. The combined data for the four particles systems considered in this study can be described in terms of the bubble size, particle properties and liquid velocity. The wake solids holdup can be described adequately through two dimensionless quantities:

$$\epsilon_{sw} = 0.52\left(\frac{Re_b}{Re_t}\right)^{1/8}(\bar{\epsilon}_s)^{5/4} \qquad [3]$$

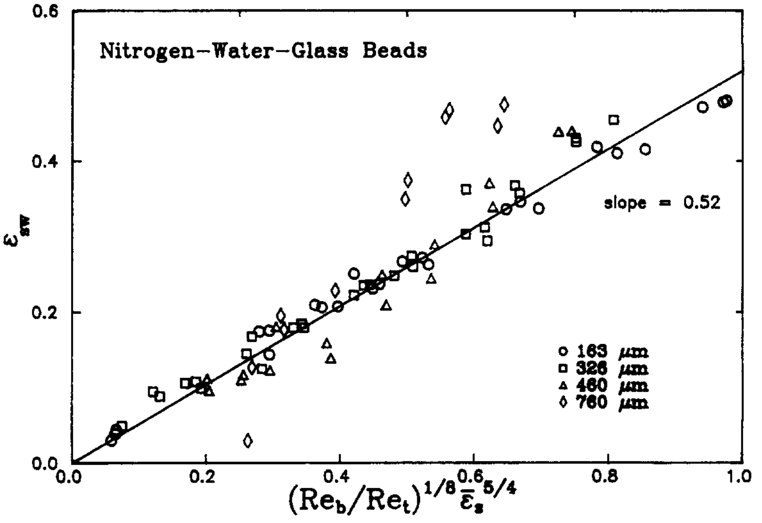

Figure 14. Correlation of the wake solids holdup (ϵ_{sw}): includes data for 163, 326, 460 and 760 μm glass beads.

or

$$X = 0.52\left(\frac{Re_b}{Re_t}\right)^{1/8}(\bar{\epsilon}_s)^{1/4}. \quad [4]$$

In [3] and [4], Re_t is the particle Reynolds number at terminal velocity defined as $\rho_p U_t d_p/\mu_L$, where d_p is the particle diameter.

Figures 14 and 15 show ϵ_{sw} and X as functions of $(Re_b/Re_t)^{1/8}$ $(\bar{\epsilon}_s)^{5/4}$ and $(Re_b/Re_t)^{1/8}$ $(\bar{\epsilon}_s)^{1/4}$, respectively. As shown, the wake solids holdup can be predicted very well by [3]. The data for the 163 and 326 μm glass beads show the best fit; those for the 760 μm glass beads show the largest deviation from the prediction, but also the largest error. In terms of X, the deviation between the predicted and experimental values is larger, but the error in the data is also magnified due to division by $\bar{\epsilon}_s$ (or ϵ_{sp}, the solids holdup in the particulate phase), a quantity < 1. Note that ϵ_{sp} is essentially identical to ϵ_s for a single bubble rising in a liquid–solid fluidized bed. The data can also be satisfactory predicted by a simple model proposed by Kreischer (1989) based on the spherical vortex concept.

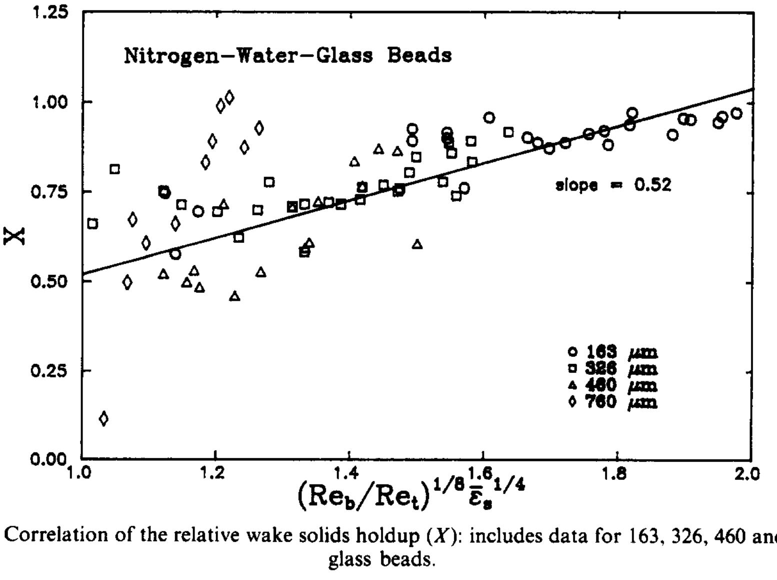

Figure 15. Correlation of the relative wake solids holdup (X): includes data for 163, 326, 460 and 760 μm glass beads.

Under most conditions in this study, the wake solids holdup was found to be lower than the corresponding results found in a two-dimensional system by Kitano & Fan (1988). This deviation arises from the difference in the definition and the resulting sensitivity of the effective wake utilized to evaluate the average solids holdup in the wake. As noted in the introduction, the effective wake is taken as the confined turbulent wake (CTW) (Fan 1989) by Kitano & Fan (1988); in the present work, it is taken as the primary wake which includes the regions of the CTW and the shedding vortical wake (SVW) (Fan 1989), although in a three-dimensional wake considered in this study, the solids holdup is relatively insensitive to the boundary of the wake defined. The wall effect in two-dimensional systems where particles tend to concentrate and flow down along the wall may also contribute to the deviation of the results by Kitano & Fan (1988) from their study.

CONCLUDING REMARKS

Several important points are immediately evident from this study: first, the optical fiber probe provides a good means of measuring the local solids holdup within a liquid–solid fluidized bed and, in particular, the local solids holdup within the bubble wake; second, the probe can be used to identify such phenomena as the liquid wake behind a bubble rising in a liquid–solid fluidized bed; and third, the ratio of the wake solids holdup to the particulate phase holdup falls between about 1 and 1/2 for the conditions covered in this study.

Important considerations to calculate the average wake solids holdup in a three-dimensional flow field include:

(i) The wake size was determined based on the wake boundary relationship of $h_w/\xi = 1.5$; extensive analysis of the wake behavior indicated that, within a reasonable range of wake sizes, including that prescribed, the average solids holdup in the wake was relatively insensitive to the chosen wake size.

(ii) An arithmetic average of data obtained from a given size bubble could adequately characterize the wake solids holdup.

Despite the limitations inherent in these assumptions, the experimental technique provides a useful method to directly measure the wake solids holdup.

The wake solids holdup and the relative wake solids holdup can be described by [3] and [4], respectively. However, extension to a multi-bubble system is necessary for direct application to the holdup prediction in a freely bubbling fluidized bed; thus, the effect of bubble–bubble interactions on the solids holdup in the wake must be considered.

Acknowledgement—This work was supported in part by Argonne National Laboratory Grant No. 83052401.

REFERENCES

Abuaf, N., Jones, O. C. & Zimmer, G. A. 1978 Optical probe for local void fraction and interface velocity measurements. *Rev. scient. Instrum.* **49,** 1090–1094.

Batchelor, G. K. 1951 Pressure fluctuations in isotropic turbulence. *Proc. Camb. phil. Soc.* **47,** 359–374.

Begovich, J. M. & Watson, J. S. 1978 Hydrodynamics characteristics of three-phase fluidized bed. In *Fluidization; Proc. 2nd Engng Fdn Conf.* (Edited by Davidson, J. F. & Kearns, D. L.), pp. 190–195. Cambridge Univ. Press, Cambs.

Bhaga, D. & Weber, M. E. 1972 Holdup in vertical two and three phase flow: part I theoretical analysis. *Can. J. chem. Engng* **50,** 323–328.

Bhatia, V. K. & Epstein, N. 1974 Three phase fluidization: a generalised wake model. In *Proc. Int. Symp. on Fluidization and Its Applications, Toulouse* (Edited by Angelino, H., Couderc, J. P., Gibert, H. & Laguerie, C.), pp. 380–382. Cepadues-Editions,

Darton, R. C. & Harrison, D. 1975 Gas and liquid holdup in three-phase fluidization. *Chem. Engng Sci.* **30,** 581–586.

DELHAYE, J. M. 1981 Gas–liquid two-phase flow in tubes. *Entropie* **99**, 3–25.

DHANUKA, V. K. & STEPANEK, J. B. 1978 Gas and liquid hold-up and pressure drop measurements in a three-phase fluidized bed. In *Fluidization*; *Proc. 2nd Engng Fdn Conf.* (Edited by DAVIDSON, J. F. & KEARNS, D. L.), pp. 179–183. Cambridge Univ. Press, Cambs.

EL-TEMTAMY, S. A. & EPSTEIN, N. 1978 Bubble wake solids content in three-phase fluidized bed. *Int. J. Multiphase Flow* **4**, 19–31.

EPSTEIN, N. 1981 Three-phase fluidization: some knowledge gaps. *Can. J. chem. Engng* **59**, 649–657.

FAN, L.-S. 1989 *Gas–Liquid–Solid Fluidization Engineering*. Butterworths, Stoneham, Mass.

HENRIKSON, H. K. & OSTERGAARD, K. 1974 On the mechanism of break-up of large bubbles in liquids and three-phase fluidised beds. *Chem. Engng Sci.* **29**, 626–629.

HETZLER, R. & WILLIAMS, M. C. 1969 Fluidized bed viscosity and expansion, correlated with glass-forming liquid model. *Ind. Engng Chem. Fundam.* **8**, 668–677.

HU, T., YU, B. & WANG, Y. 1986 Holdups and models in three phase fluidized beds. In *Proc. 5th Engng Fdn Conf. on Fluidization*, Elsinore, Denmark, pp. 353–360.

ISHIDA, M. & TANAKA, H. 1982 An optical probe to detect both bubbles and suspended particles in a three-phase fluidized bed. *J. chem. Engng Japan* **15**, 389–391.

JEAN, R. H. & FAN, L.-S. 1987 Bed contraction criterion for three phase fluidization. *Can. J. chem. Engng* **65**, 351–352.

KITANO, K. & FAN, L.-S. 1988 Near wake structure of a single gas bubble in a two-dimensional liquid–solid fluidized bed: solids holdup. *Chem. Engng Sci.* **43**, 1355–1361.

KOJIMA, E., AKEHATA, T. & SHIRAI, T. 1975 Behavior of single air bubbles held stationary in downward flows. *J. chem. Engng Japan* **8**, 108–113.

KREISCHER, B. E. 1989 Bubble and bubble wake characteristics in a gas–liquid–solid fluidized bed. Ph.D. Dissertation, The Ohio State Univ., Columbus.

DE LASA, H. I., LEE, S. L. P. & BERGOUGNOU, M. A. 1984 Bubble measurement in three-phase fluidized beds using a U shape optical fiber. *Can. J. chem. Engng* **62**, 165–169.

LEE, S. L. P. & DE LASA, H. I. 1986 Characterization of bubbles in three phase fluidized beds using U-shaped optical fiber probes. In *Proc. 5th Engng Fdn Conf. on Fluidization*, Elsinore, Denmark, pp. 361–368.

LEE, S. L. P., DE LASA, H. I. & BERGOUGNOU, M. A. 1984 Bubble phenomena in three-phase fluidized beds as viewed by a U-shaped fiber optic probe. *AIChE Symp. Ser.* **80**(241), 110–116.

MICHELSEN, M. L. & OSTERGAARD, K. 1970 Holdup and fluid mixing in gas–liquid fluidised beds. *Chem. Engng J.* **1**, 37–45.

MIYAHARA, T., TSUCHIYA, K. & FAN, L.-S. 1988 Wake properties of a single gas bubble in a three-dimensional liquid–solid fluidized bed. *Int. J. Multiphase Flow* **14**, 749–763.

PRUDEN, B. B. & EPSTEIN, N. 1964 Stratification by size in particulate fluidization and in hindered settling. *Chem. Engng Sci.* **14**, 696–700.

RICHARDSON, J. F. & ZAKI, W. N. 1954 Sedimentation and fluidisation: part I. *Trans. Instn chem. Engrs* **32**, 35–53.

TSUCHIYA, K. & FAN, L.-S. 1988 Near-wake structure of a single gas bubble in a two-dimensional liquid–solid fluidized bed: vortex shedding and wake size variation. *Chem. Engng Sci.* **43**, 1167–1181.